Çukurova Üniversitesi Mühendislik Mimarlık Fakültesi Dergisi, 33(3), ss. 245-254, Eylül 2018
Çukurova University Journal of the Faculty of Engineering and Architecture, 33(3), pp. 245-254, September 2018

Microstrip Patch Antennas Covered with Chiral Metamaterial Structures

Mehmet BAĞMANCI[1], Muharrem KARAASLAN[1], Emin UNAL[1], Faruk KARADAG[*2]

[1]Iskenderun Technical University, Department of Electrical and Electronics Engineering, Iskenderun, Hatay,
[2]Cukurova University, Art and Science Faculty, Department of Physics, Adana

Geliş tarihi: 16.05.2018 Kabul tarihi: 15.10.2018

Abstract

In this working we present gain characteristic of microstrip patch antennas covered with chiral metamaterial. In order to determine gain of antennas covered with chiral metamaterial structure, S11 parameters and radiation pattern of antennas with chiral metamaterial and without chiral metamaterial are plotted and compared each other. The simulation results show that antennas covered with chiral metamaterial structure increase either gain or radiation pattern or both at operation frequency.

Keywords: Gain patch antenna, metamaterial, chiral metamaterial, antennas covered with chiral metamaterial

Bakışımsız Metamalzeme Kaplı Mikroşerit Anten Yapıları

Öz

Bu çalışmada bakışımsız metamalzeme kaplı mikroşerit antenlerin kazanç karakteristiği ortaya koyulmuştur. Bakışımsız metamalzeme kaplı mikroşerit antenin kazancını belirlemek için, metamalzeme kaplı yüzeyin bakışımısız mtamalzemeli ve bakışımsız metamalzemesiz sonuçları grafiğe dökülmüş ve bunlar yorumlanarak birbiriyle karşılaştırılmıştır. Simulasyon sonuçları bakışımsız metamalzeme kaplı antenin kazancının ve yayılım patentinin arttığını ortaya göstermiştir.

Anahtar Kelimeler: Yama anten kazancı, Mikroşerit anten, Bakışımsız metamalzeme, Bakışımsız metamalzemeli antenler

[*]Sorumlu yazar (Corresponding author): Faruk KARADAĞ, *fkaradag@cu.edu.tr*

1. INTRODUCTION

In recent years microstrip patch antennas is widely used many areas such as space crafts, aircrafts, radars, satellite communications, and guided missile etc. owing to easiness of using and fabrication and low cost. Whereas it has many advantages as mentioned, it has some disadvantages, which result from dielectric and conductor losses. In addition, gain diminution and inadequate directivity are also observed in this antenna due to surface waves [1]. By using low loss dielectric substrate and perfect conductor, dielectric and conductor losses can be reduced minimum levels. But using low loss dielectric substrate and perfect electric conductors results in higher manufacture cost. Gain, downscaling, bandwidth improvement and broad band directivity can be ensured by using metamaterial structures [2-6]. Metamaterials has had increasing attention in recent years due to their unusual properties that cannot be found in nature. First time, Veselago studied on the conditions to get negative refractive index and he suggested in 1968 that having negative permittivity (ε) and negative permeability (μ) is possible simultaneously [7].

Pendry put these new and extraordinary materials in practice in 1999 [8], after Veselago's discoveries. These unusual and exciting properties of metamaterials usher new age for various applications medicine to military. Some of these applications are negative refraction [9,10], polarization rotation, energy harvesting [11], super lenses [12,13], perfect absorption [14-17], invisibility cloaking [18-20], sensing [21] etc.

Metamaterials have also many scopes of application for new antenna systems [22-25]. One of the important technic of metamaterials is downscaling of the microstrip antennas with different types of artificial materials. The common method of reducing the antenna size is using high permittivity substrate. This way diminishes the wavelength of the signal in the substrate [26]. But, due to high permittivity, energy consumption of antenna becomes more, since high permittivity decreases the impedance bandwidth of the antenna. Another method is removing the substrate in order to reduce the effective dielectric constant to minimum value. This method compels the wave to travel in the substrate, so gain of patch antenna has been increases [27,28]. But this gain increment is about 2 dB which is maximum value with all this mentioned techniques and directivity change too little. In order to make a success of these problems, many different solutions have been proposed. Usage of metamaterials with patch antennas is one of these solutions [29-32].

In this article, a way is proposed to enhance both the gain and directivity of patch antenna. Simulations are conducted three different microstrip antenna patched with three different chiral metamaterial structures. For each antenna chiral metamaterial structure responsible for negative permittivity and negative permeability which improve not only gain but also directivity of microstrip patch antenna. The effective permittivity and permeability of SRRs were evaluated by using finite difference time domain method (FDTD) based computer CST (Computer Simulation Technology) Microwave Studio. The dimensions of chiral metamaterial of three structures are optimized by using neural network in order to find out negative values for the constitutive parameters (z, n) at the operation frequency of microstrip patch antenna. Chiral metamaterials have been situated on microstrip patch antenna to see the effects of the chiral metamaterial on microstrip patch antenna. Simulation results are compatible with constitutive parameters of chiral metamaterial structure. It can be seen next sections that chiral metamaterials significantly improve gain of the microstrip patch antennas.

2. DESIGNING OF ANTENNAS WITH CHIRAL METAMATERIALS

2.1. Antenna Patched with First Chiral Metamaterial Structure

First chiral metamaterial consists of a square-shaped resonator with gaps the unit cell and the same shaped rotated 15° on other side. Dimensions

and front view of the designed chiral metamaterial (MTM) structure are shown in Figure 1(a). Back and side views of designed chiral MTM structure are demonstrated in Figure 1 (b) and (c), respectively. Dimensions of unit-cell are given in Table 1. FR-4 and copper are used in simulations as dielectric substrate and metal film. Dielectric permittivity and loss tangent of chosen FR-4 are 4.2 and 0.02, respectively. The metal films are selected as copper (electric conductivity of 5.8x107 S/m) [33]. Dimensions of chiral MTM structure are optimized by using neural network to get negative permittivity and permeability simultaneously at operation frequencies of microstrip patch antenna (4.41 GHz and 5.36 GHz). The chiral MTM is simulated and analysed with a commercial full-wave electromagnetic solver (CST Microwave Studio) based on FIT (finite integration technique). In the simulations boundary conditions are arranged unit cell for x and y directions and open (add space) for z directions [33]. The constitutive parameters can be evaluated by using scattering parameters (S11 and S21) with the help of Nicolson Ross Weir (NRW) approximation [34,35],

$$\varepsilon(\text{eff})=\frac{n}{z} \quad (1)$$

$$\mu(\text{eff})=n*z \quad (2)$$

$$z=\sqrt{\frac{(1+S11)^2-S21^2}{(1-S11)^2-s21^2}} \quad (3)$$

$$n=\frac{j}{k0*d}\ln\left(\frac{S21}{1-S11*\frac{z-1}{z+1}}\right) \quad (4)$$

In Equation 1 and 2; n, ε(eff) and μ(eff) represent refractive index, effective permittivity and effective permeability, correspondingly. In equation 4, k_0, d and z symbolized the free space wave number, thickness of metamaterial and impedance, respectively. The operation frequency of antenna with chiral metamaterial structure is between 4 GHz and 6 GHz. Constitutive parameters (n, ε(eff) and μ(eff)) have negative values at 4.41 GHz and 5.36 GHz. So, this chiral structure can be used as negative refractive index metamaterial with patch antenna at these operation frequencies. Constitutive parameters are demonstrated in Figure 2.

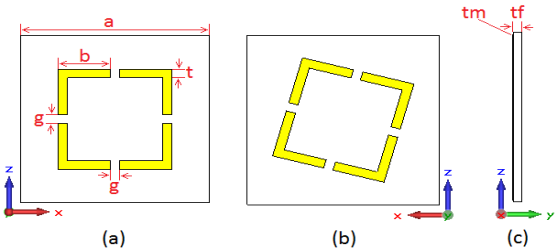

Figure 1. (a) Designed Chiral mtm (a) dimension and front view, (b) back view and (c) side view

Table 1. Typical size of proposed Chiral MTM structure

Parameter	a	b	t	g	tf	tm
Value (mm)	40	11	2	2	0,036	1,6

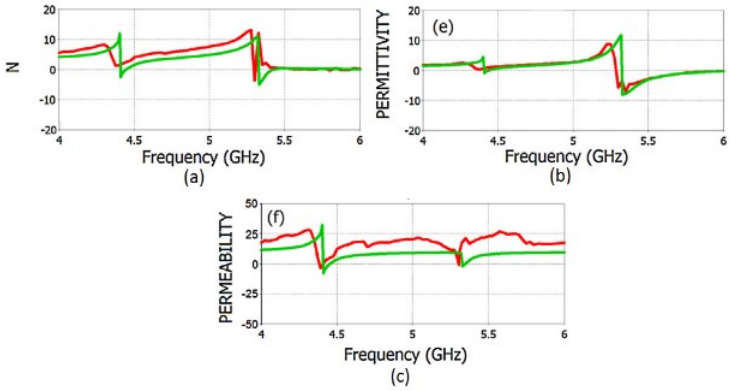

Figure 2. Constitutive parameters of structure (a) n, (b) ε(eff) and (c) μ(eff)

Microstrip patch antenna has designed in accordance with chiral metamaterial's operation frequency in which refractive index, permittivity and permeability are negative. In this paper one of two operation frequency of chiral metamaterial is chosen as operation frequency for microstrip patch antenna. Microstrip patch antenna and dimensions of microstrip patch antenna are demonstrated in Figure 3 and Table 2, respectively. Thickness of dielectric layer and metal layers of microstrip patch antenna are tf and tm, correspondingly which are identical with chiral metamaterial's dielectric and metal layers thickness. FR-4 is used as dielectric substrate (dielectric permittivity and loss tangent of chosen FR-4 are 4.2 and 0.02, respectively). The metal layers are selected as copper (electric conductivity of 5.8x107 S/m). The numerical simulations are done with CST Microwave studio. Dimensions demonstrated in Table 2 are optimum values of microstrip patch antenna for operation frequency (5.36 GHz)

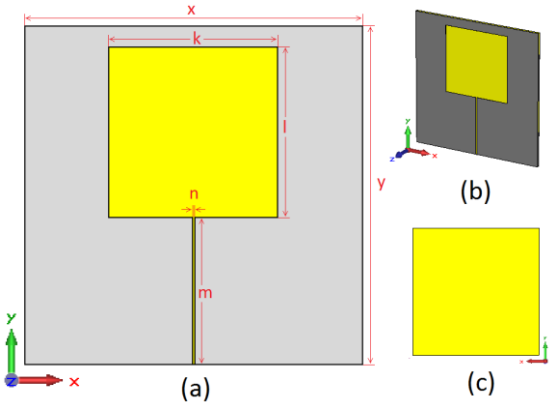

Figure 3. Designed microstrip patch antenna (a) dimension and front view, (b) perspective view and (c) back view

Table 2. Dimensions of microstrip patch antenna

Parameter	x	y	k	l	m	n	tf	tm
Value (mm)	78	78	39.15	39.15	33.85	0.5	0.035	1.6

In order to enhance the gain of microstrip patch antenna the direction of metamaterial is important due to anisotropic behaviour of chiral metamaterial. So, chiral metamaterial has been placed on centre of antenna which is shown Figure 4. The numeric simulations of microstrip patch antenna with chiral metamaterial and without chiral metamaterial are demonstrated in Figure 5. In Figure 5, reflection coefficient (S11) -26 dB and -9.74 dB at 5.36 GHz for microstrip patch antenna without and with chiral metamaterial structure. It can be seen that reflection coefficient is increased up 7.6 dB with mounting of chiral metamaterial structure on microstrip patch antenna. Although there is no increase the gain of antenna, radiation pattern of antenna with chiral metamaterial is quite satisfactory.

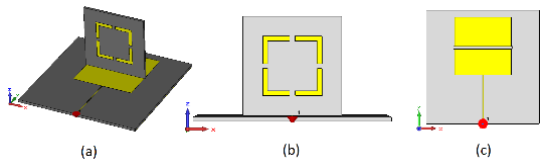

Figure 4. Microstrip patch antenna with chiral metamaterial structure (a) perspective view, (b) bottom view and (c) front view

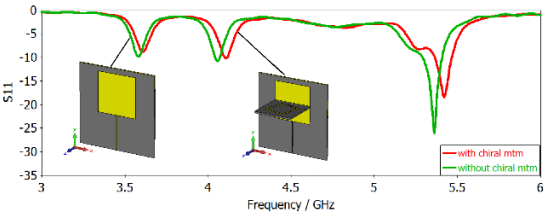

Figure 5. S_{11} parameters of microstrip patch antenna with and without chiral metamaterial

Since only the return loss (reflection coefficient (S11)) is not enough to decide the output of antenna, radiation pattern of microstrip patch antenna with and without chiral metamaterial is need to be studied to understand gain of microstrip patch antenna. The radiation pattern of microstrip patch antenna with and without chiral metamaterial are evaluated at 5.36 GHz for 90° Φ (phi) angle which are shown in Fig. 6. In Figure 6, it is clearly seen that main lobe magnitude increase from 11.3 dB to 11,6 dB and angular width increase from 31.8 ° to 32°. In addition, this, in Figure 7, absolute value of radiation pattern is simulated at every 30° between 0°-90°. The value of main lobe magnitude, angular with (3 dB) and side lobe level

for different Φ angle are presented in Table 3. It can be seen in Table 3 that good results have not been gotten in terms of angular width (3dB) and side lobe level at value of lower Φ angle (0º and 30º) for microstrip patch antenna with chiral metamaterial, but at higher degrees (60º and 90º) main lobe magnitude, side lobe level and angular width of antenna with chiral metamaterial better than antenna without chiral metamaterial.

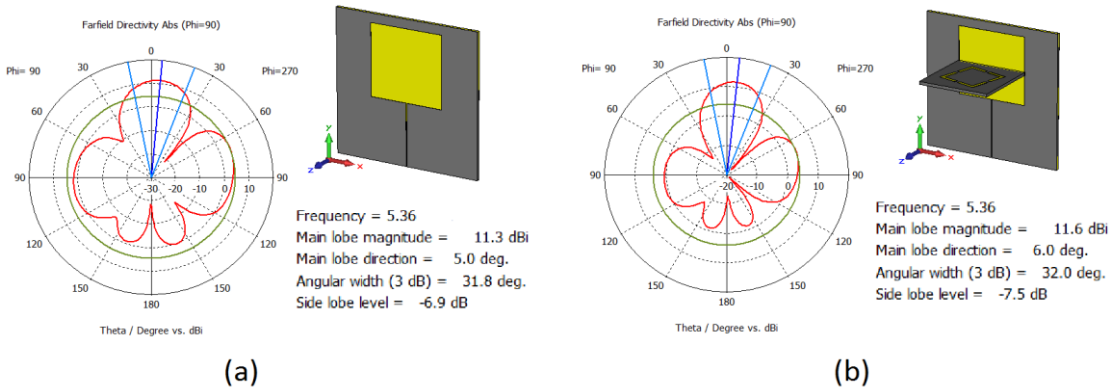

Figure 6. Absolute value of radiation pattern of microstrip patch antenna (a) without chiral metamaterial and (b) with chiral metamaterial

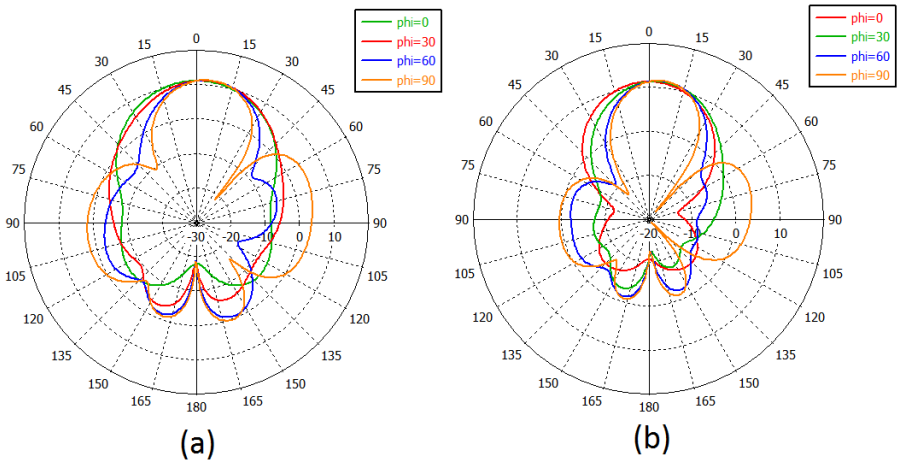

Figure 7. Radiation pattern of microstrip patch antenna for different Φ (phi) angle (a) without chiral metamaterial and (b) with chiral metamaterial

Table 3. Comparison of radiation pattern of microstrip patch antenna with and without chiral metamaterial for different angle

	Without mtm					**With mtm**			
Φ (Phi)	**0º**	**30º**	**60º**	**90º**		**0º**	**30º**	**60º**	**90º**
Main lobe magnitude(dB)	11	11.2	11.3	11.3		11.3	11.4	11.6	11.6
Angular width- 3 dB (deg)	50.7	44.6	35.1	31.8		48.6	43.7	35.2	32
Side lobe level (dB)	-17.3	-14.9	-12.1	-6.9		-17.2	-14.6	-13	-7.5

2.2. Antenna Patched with Second Chiral Metamaterial Structure

The suggested second chiral metamaterial structure consists of discontinuous bilayer cross-wire-shapes and rotated wire strips separated by a dielectric substrate as shown in Figure 8. FR4 is chosen as the dielectric substrate and the metallic pattern is modelled as a copper sheet with an electrical conductivity of 5.8x107 S/m and thickness of 0.0035 mm. The thickness, relative permittivity and loss tangent of FR4 are 1.6 mm, 4.2 and 0.02, respectively. The unit cell dimensions of the second chiral metamaterial structure are demonstrated in Table 4 and other dimensions are shown in Figure 8 (a). The angle parameters of the structures are given as 45º for the front side of the structure and 75º for the back of the structure with respect to the origin [36]. Dimensions of chiral MTM structure are optimized by using neural network to get negative permittivity and permeability simultaneously at operation frequencies of microstrip patch antenna (6.6 GHz and 8.3 GHz). The simulation of the periodic structure was performed with a commercial full-wave EM solver based on the finite integration technique. The unit cell boundary conditions were applied to a single-unit cell in the simulation [36]. In Figure 9, chirality (n), permittivity (ε) andpermeability (μ) of second chiral metamaterial structure for two different thickness of wire (w=0.25 mm and w=30 mm). In this work, we use chiral structure whose wire thickness = 0.25 mm.

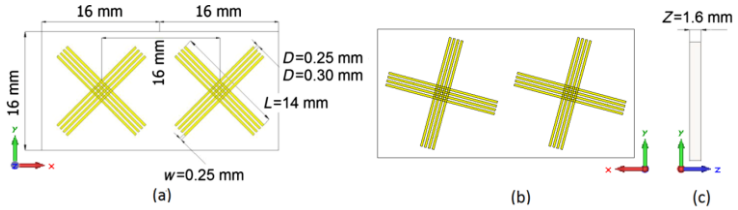

Figure 8. Designed second chiral mtm (a) dimension and front view, (b) rear view and (c) side view

Table 3. Typical size of second Chiral MTM structure

Parameter	w	L	D	Z	Metal thickness
Value (mm)	0.25	14	0.25	1.6	0.035

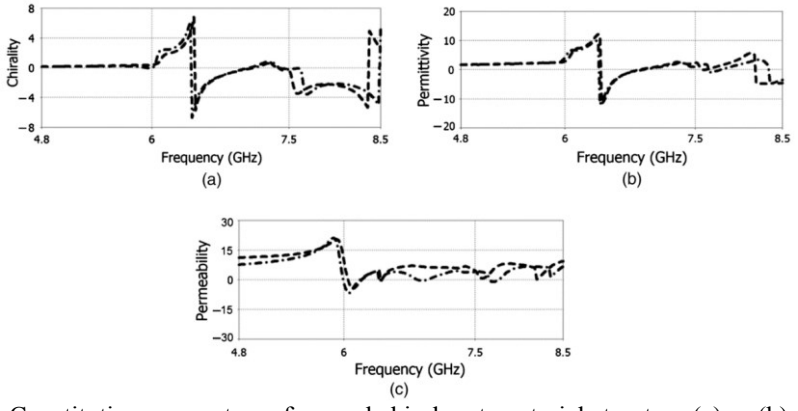

Figure 9. Constitutive parameters of second chiral metamaterial structure (a) n, (b) εand (c) μ

Second microstrip patch antenna has designed in compatible with second chiral metamaterial's operation frequency where chirality, permittivity and permeability are negative. In this section one

of two operation frequency of chiral metamaterial is chosen as operation frequency for microstrip patch antenna which is 8.3 GHz. Designed microstrip patch antenna is shown in Figure 10. Dimensions of second microstrip patch antenna are presented in Table 5. FR-4 is used as dielectric substrate (dielectric permittivity and loss tangent of chosen FR-4 are 4.2 and 0.02, respectively). The metal layers are selected as copper (electric conductivity of 5.8x107 S/m). The numerical simulations are done with CST Microwave studio. Dimensions are shown Table 5 is optimal value of antenna for operation frequency.

As in the first microstrip patch antenna, chiral metamaterial structure has been placed on centre of antenna due to anisotropic behaviour of chiral metamaterials, because the direction of chiral metamaterial is significant to increase the gain of microstrip patch antenna. In Figure 11 microstrip patch antenna mounted with chiral metamaterial structure is demonstrated. The simulation results of second microstrip patch antenna with and without chiral metamaterial are shown in Figure 12. In Figure 12, return loss (S11) -13, 57 dB at 8.3 GHz for antenna without chiral metamaterial and -15.71 dB at 8.33 GHz for antenna with chiral metamaterial structure. It is clearly seen that return loss (S11) is decreased down 1.97 dB with situating of chiral metamaterial structure on microstrip patch antenna. In addition, next step radiation pattern of antenna without and with chiral metamaterial is investigated to better understand gain characteristic of antenna.

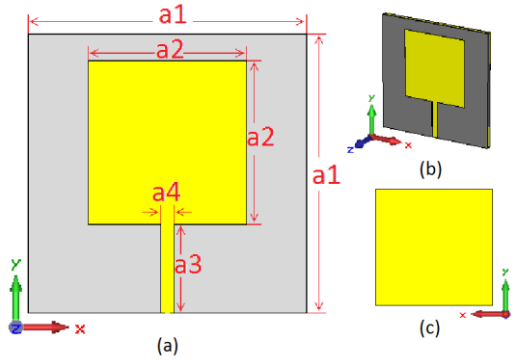

Figure 10. Designed second microstrip patch antenna (a) dimension and front view, (b) perspective view and (c) back view

Table 5. Dimensions of second microstrip patch antenna

Parameter	**a1**	**a2**	**a3**	**a4**
Value (mm)	78	78	39.15	39.15
Other (mm)	**Substrate thickness:**	1.6	**Copper thickness:**	0.035

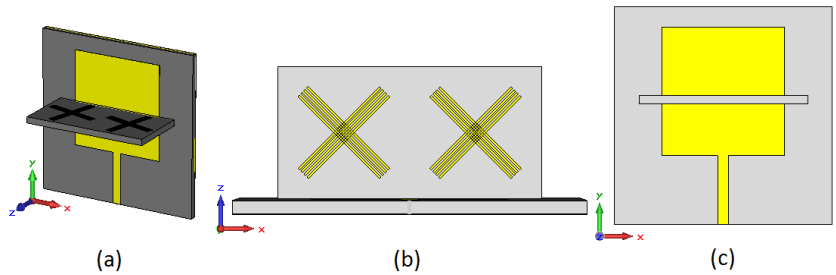

Figure 11. Microstrip patch antenna with chiral metamaterial structure (a) perspective view, (b) bottom view and (c) front view

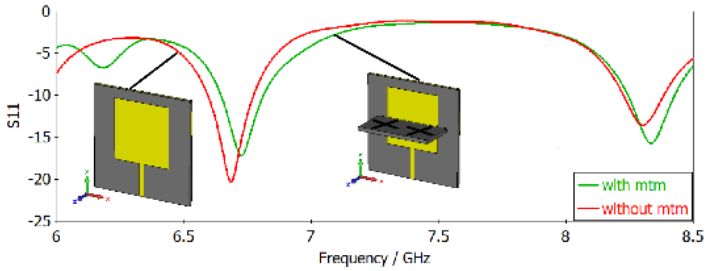

Figure 12. S_{11} parameters of second microstrip patch antenna with and without chiral metamaterial

Due to the fact that return loss (S11) give us insufficient information about gain of antenna, we decide to investigate radiation pattern of second microstrip patch antenna with and without chiral metamaterial. Firstly, the radiation pattern of microstrip patch antenna with and without chiral metamaterial are evaluated at chiral frequency (8.3 GHz) for 90º Θ (theta) angle which are demonstrated in Figure 13. When we look Figure 13, we can see that main lobe magnitude increase from 2.58 dB to 2.95 dB which is correspond to 0,37 dB.

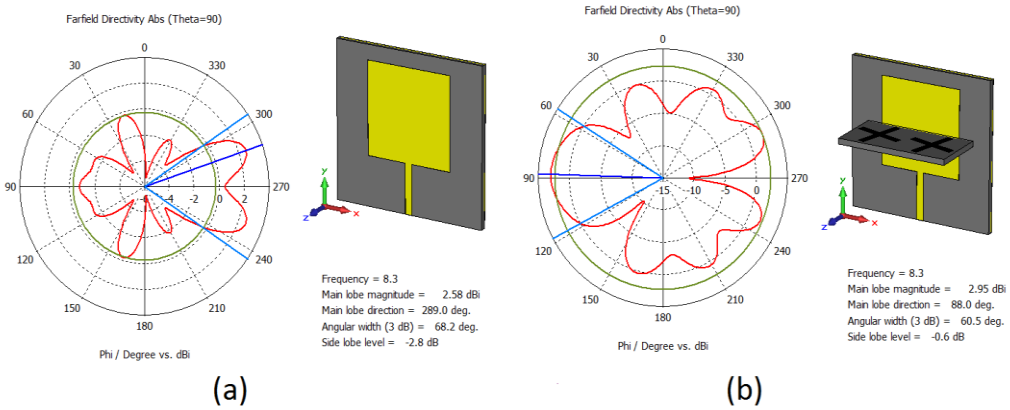

Figure 13. Absolute value of radiation pattern of second microstrip patch antenna for theta angle (a) without chiral metamaterial and (b) with chiral metamaterial

3. CONCLUSION

In summary, we show gain characteristic of microstrip patch antennas covered with chiral metamaterial structure. In numeric simulations S_{11} parameters and radiation pattern of antennas with and without chiral metamaterial structure are compared each other to determine gain of antennas covered with chiral metamaterial structure. The numeric results show that antennas covered with chiral metamaterial structure increase gain or radiation pattern or both at working frequency. In numeric simulations, main lobe magnitude of microstrip patch antenna has been increased from 11.3 Db to 11.6 dB using first chiral structure. Second chiral structure has decreased return loss parameters (S_{11}) of microstrip patch antenna from -13.57 dB to -15.71 dB which is correspond 1.97 dB. We can say that microstrip patch antennas covered with chiral metamaterial structures are good candidate for antennas applications

4. REFERENCES

1. Waterhouse, R., 2003. Micro Strip Patch Antennas, A Designer's Guide, Kluwer Academic Publishers, Boston, MA.

2. Jafargholi, A., Manouchehr K., 2012. Dipole Antenna Miniaturization Using Single-Cell Metamaterial, Applied Computational Electromagnetics Society Journal, 27, 3.

3. Palandoken, M., Grede, A., Henke, H., 2009. Broadband Microstrip Antenna with Left-handed Metamaterials, IEEE Transactions on Antennas and Propagation, 57(2), 331-338.

4. Veysi, M., Jafargholi, A., 2012. Directivity and Bandwidth Enhancement of Proximity-Coupled Microstrip Antenna using Metamaterial Cover, Applied Computational Electromagnetics Society Journal, 27, 11.

5. Burokur, S.N., Latrach, M., Toutain, S., 2005. Theoretical Investigation of a Circular Patch Antenna in the Presence of a Left-handed Medium, IEEE Antennas and Wireless Propagation Letters, 4:183-186.

6. Tao, L., Xiang-Yu, C., Yun, G., Qun Yang Wen-Qiang, Li., 2011. Design of Miniaturized Broadband and High Gain Metamaterial Patch Antenna, Microwave and Optical Technology Letters, 53.12: 2858-2861.

7. Veselago, V.G., 1968. The Electrodynamics of Substances with Simultaneously Negative Values of and μ, Soviet Physics Uspekhi, 10(4), 509.

8. Pendry, J.B., Holden, A.J., Robbins, D.J., Stewart, W.J., 1999. Magnetism from Conductors and Enhanced Nonlinear Phenomena, IEEE Transactions on Microwave Theory and Techniques, 47.11: 2075-2084.

9. Shelby, R.A., Smith, D.R., Schultz, S., 2001. Experimental Verification of a Negative Index of Refraction, Science, 292(5514), 77-79.

10. Smith, D.R., Pendry, J.B., 2004. Wiltshire, Mike CK. Metamaterials and Negative Refractive Index, Science, 305(5685), 788-792.

11. Unal, E., Dincer, F., Tetik, E., Karaaslan, M., Bakir, M., Sabah, C., 2015. Tunable Perfect Metamaterial Absorber Design Using the Golden Ratio and Energy Harvesting and Sensor Applications, Journal of Materials Science: Materials in Electronics, 26(12), 9735-9740.

12. Pendry, J.B., 2000. Negative Refraction Makes a Perfect Lens, Physical Review Letters, 85(18), 3966.

13. Garcia, N., Nieto, V.M., 2002. Left-handed Materials do not Make a Perfect Lens, Physical Review Letters, 88(20), 207403.

14. Dincer, F., Akgol, O., Karaaslan, M., Unal, E., Demirel, E., Sabah, C., 2014. Perfect Metamaterial Absorber with Polarization and Incident Angle Independencies Based on Ring and Cross-wire Resonators for Shielding and a Sensor Application, Optics Communications, 322: 137-142.

15. Dincer, F., Akgol, O., Karaaslan, M., Unal, E., Demirel, E., Sabah, C., 2014. Polarization and Angle Independent Perfect Metamaterial Absorber Based on Discontinuous Cross-wire-strips, Journal of Electromagnetic Waves and Applications, 28(6), 741-751.

16. Dincer, F., Akgol, O., Karaaslan, M., Unal, E., Sabah, C., 2014. Design of Polarization- and Incident Angle-Independent Perfect Metamaterial Absorber with Interference Theory, Journal of Electronic Materials, 43, 11.

17. Dincer, F., Akgol, O., Karaaslan, M., Unal, E., Sabah, C., 2014. Polarization Angle Independent Perfect Metamaterial Absorbers for Solar Cell Applications in the Microwave, Infrared, and Visible Regime, Progress in Electromagnetics Research, 144, 93-101.

18. Cummer, S.A., Ioan Popa, B., Schurig, D., Smith, D.R., 2006. Full-wave Simulations of Electromagnetic Cloaking Structures, Physical Review E, 74(3), 036621.

19. Cai, W., Chettiar, U.K., Kildishev, A.V., Shalaev, V.M., 2007. Optical Cloaking with Metamaterials, Nature Photonics, 1(4), 224-227.

20. Schurig, D., Mock, J.J., Justice, B.J., Cummer, S.A., Pendry, J.B., Starr, A.F., Smith, D.R., 2006. Metamaterial Electromagnetic Cloak at Microwave Frequencies. Science, 314(5801), 977-980.

21. Karaaslan, M., Bakır, M., 2014. Chiral Metamaterial Based Multifunctional Sensor Applications, Progress in Electromagnetics Research, 149, 55-67.

22. Abdouni, W., Tarot, A.C., Sharaiha, A., 2008. Realisation of a Compact Patch Antenna over an Artificial Magneto-dielectric Substrate, ACES 2008 the 24th Annual Review of

Progress Applied Computational Electromagnetics.

23. Tang, M.C., Xiao, S., Wang, D., Xiong, J., Chen, K., Wang, B., 2011. Negative Index of Reflection in Planar Metamaterial Composed of Single Split-ring Resonators, Applied Computational Electromagnetics Society Journal 26(3), 250-258.

24. Fazi, C., Shi, S., Mirza, I., Prather, D., 2007. Split Ring Resonator Slab Modelling for a Metamaterial Loaded Loop Antenna, 23rd Annual Review of Progress in Applied Computational Electromagnetics (ACES), Verona, Italy, 117-122.

25. Liu, J.C., Shao, W., Wang, B.Z., 2011. A Dual-band Metamaterial Design Using Double SRR Structures, Applied Computational Electromagnetics Society Journal, 26(6), 459-463.

26. Szabo, Z., Park, G., Hedge, R., Er-Ping, Li., 2010. A Unique Extraction of Metamaterial Parameters Based on Kramer's–Kronig Relationship, IEEE Transactions on Microwave Theory and Techniques 58(10), 2646-2653.

27. Hwang, R.B., Peng, S.T., 2003. Surface-wave Suppression of Resonance-type Periodic Structures, IEEE Transactions on Antennas and Propagation, 51(6), 1221-1229.

28. Lo, Y.T., Solomon, D., Richards, W., 1979. Theory and Experiment on Microstrip Antennas, IEEE Transactions on Antennas and Propagation 27(2), 137-145.

29. Colburn, J.S., Rahmat-Samii, Y., 1999. Patch Antennas on Externally Perforated High Dielectric Constant Substrates, IEEE Transactions on Antennas and Propagation 47(12), 1785-1794.

30. Ikonen, P., Maslovski, S., Tretyakov, S., 2005. PIFA Loaded with Artificial Magnetic Material: Practical Example for Two Utilization Strategies, Microwave and Optical Technology Letters 46(3) 205-209.

31. Yeap, S.B., Chen, Z.N., 2010. Microstrip Patch Antennas with Enhanced Gain by Partial Substrate Removal, IEEE Transactions on Antennas and Propagation 58(9), 2811-2816.

32. Mosallaei, H., Sarabandi, K., 2004. Antenna Miniaturization and Bandwidth Enhancement Using a Reactive Impedance Substrate, IEEE Transactions on Antennas and Propagation 52.9: 2403-2414.

33. Dincer, F., Karaaslan, M., Akgol, O., Unal, E., Sabah, C., 2015. Dynamic and Tuneable Chiral Metamaterials with Wideband Constant Chirality Over a Certain Frequency Band, Optik-International Journal for Light and Electron Optics, 126(24), 4808-4812.

34. Weir, W.B., 1974. Automatic Measurement of Complex Dielectric Constant and Permeability at Microwave Frequencies, Proceedings of the IEEE, 62(1), 33-36.

35. Nicolson, A.M., Ross, G.F., 1970. Measurement of the Intrinsic Properties of Materials by Time-domain Techniques, IEEE Transactions on Instrumentation and Measurement, 19(4), 377-382.

36. Dincer, F., Karaaslan, M., Unal, E., Akgol, O., Sabah, C., 2014. Chiral Metamaterial Structures with Strong Optical Activity and Their Applications, Optical Engineering, 53(10), 107101-107101.